Harrison LM, Dunning SA, Woodward J, Davies TRH.

Post rock-avalanche dam outburst flood sedimentation in Ram Creek, Southern Alps, New Zealand.

*Geomorphology* 2015, 241, 135-144.



**Link to published version of article:**

http://dx.doi.org/10.1016/j.geomorph.2015.03.038

**Date deposited:**

06/10/2015

**Embargo release date:**

17 April 2016

Accepted Manuscript

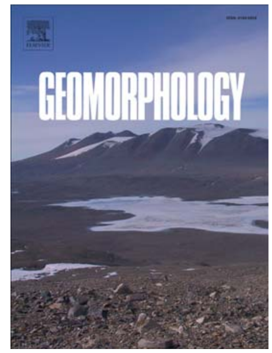


# Post rock-avalanche dam outburst flood sedimentation in Ram Creek, Southern Alps, New Zealand

Lisa Harrison, Stuart A. Dunning, John Woodward, Timothy R.H. Davies

PII: S0169-555X(15)00206-8
DOI: doi: 10.1016/j.geomorph.2015.03.038
Reference: GEOMOR 5175

To appear in: *Geomorphology*

Received date: 10 September 2014
Revised date: 23 March 2015
Accepted date: 30 March 2015

Please cite this article as: Harrison, Lisa, Dunning, Stuart A., Woodward, John, Davies, Timothy R.H., Post rock-avalanche dam outburst flood sedimentation in Ram Creek, Southern Alps, New Zealand, *Geomorphology* (2015), doi: 10.1016/j.geomorph.2015.03.038

# Post rock-avalanche dam outburst flood sedimentation in Ram Creek, Southern Alps, New Zealand

**Lisa Harrison [a], Stuart A. Dunning [a*], John Woodward [a], Timothy R. H. Davies [b]**

[a] Department of Geography, Northumbria University, Ellison Place, Newcastle Upon Tyne, United Kingdom, NE1 8ST.
[b] Department of Geological Sciences, University of Canterbury, Christchurch, New Zealand.

* Corresponding author. Tel.: +44 191 227; E-mail: stuart.dunning@northumbria.ac.uk

**Abstract**

Rock avalanches are common in mountainous regions that are tectonically active. They are capable of forming natural dams of uncertain persistence that have significant impacts on the river system over wide spatial scales and possibly over geological time scales. Here we combine field data and digital elevation model (DEM) analysis to show the response of Ram Creek, New Zealand, to 28 years of sediment dispersion following the 1968 emplacement of a co-seismic, rock-avalanche dam that breached catastrophically in 1981. The results show a system that has not attained equilibrium, being unable to move the quantity of dam-derived sediments, and will likely not attain equilibrium before the next major sediment input; it is in a state of persistent disturbance where localised reworking dominates. Erosion in Ram Creek is focussed on lateral bevelling and bedrock gorge widening rather than vertical incision to keep pace with tectonic uplift. Importantly for studies of tectonic geomorphology, this widening — which if sustained will form a strath terrace — does not represent a period of reduced uplift. Stream metrics (concavity and steepness) are unable to differentiate the identified rock-avalanche–induced knickpoint from tectonic and lithological knickpoints.

*Keywords:* rock avalanche; landslide dam; river metrics; strath formation; New Zealand

## 1. Introduction

In tectonically active mountain environments, catastrophic mass movements — often associated with seismic triggering — can control valley floor geomorphology far beyond the failure site (Pearce and Watson, 1986 ;Hewitt, 1999, 2006; Korup, 2005a**;** Korup et al., 2004). It is becoming ever more apparent that large landslide deposits can exert a dominant geomorphic control on the fluvial system (Burbank et al., 1996; Montgomery and Brandon, 2002; Korup, 2005b; Korup et al., 2009, 2010;).

Rock avalanches (RAs) are a high-magnitude, low-frequency mechanism of eroding mountain peaks and delivering sediment to valley floors (Hovius et al., 1997; McSaveney, 2002). They commonly involve a minimum volume of ~1 x $10^6$ $m^3$ of rock and associated cover, which are transported from a discrete source to the valley floor at speeds of 100-250 km/h. In actively incising systems with narrow valleys, they can immediately block a river valley with a highly compact deposit (Hewitt, 1999, 2009; Dunning et al., 2005, 2006; Hewitt et al., 2008). These natural dams can last anywhere from minutes to millennia, posing significant hazard to life and infrastructure (Dunning et al., 2006) and provoking a geomorphic response at varied temporal and spatial scales in fluvial and hillslope systems (Costa and Schuster, 1988; Hewitt, 2006). The RAs supply an abnormal point-load of sediment to the fluvial system as opposed to the distributed, chronic, delivery of smaller landslides. This increases the volume of sediment storage within a catchment as rivers are often forced into a transport-limited state (Adams, 1980; Pearce and Watson, 1986; Korup et al., 2004, 2010; Korup, 2005b; Hewitt, 2006, 2009).

During RA emplacement, intact bedrock is broken apart by brittle fracture, pulverisation, and crushing. This creates distinctive rock-avalanche deposits (RADs) comprised of poorly sorted, angular to very angular clasts of gravel, sand, and (mostly) finer grades with small-scale agglomerates, capped by a boulder carapace (Davies et al., 1999; McSaveney, 2002; Dunning et al., 2006; Mitchell et al., 2007; Hewitt et al., 2008; Hewitt, 2009; Reznichenko et al., 2011). Beneath the coarse surface and near-surface carapace, the bulk of the deposit is therefore composed of bedrock fragmented to sizes finer than the 'normal' bedload of many rivers in mountainous regions.

Rock-avalanche dams can overtop and remain stable, (Hewitt, 1998), or breach with stable overflow channel allowing the majority of dam volume to persist. The RADs often persist after overtopping because of self-armouring of the breach channel by the coarse carapace falling into the developing breach channel sides (Dunning et al., 2006). However, if an RA dam breaches and fails catastrophically, the resultant outburst floods are capable of mobilising large volumes of the RA sediment and (if present) impounded lake sediments, rapidly and widely dispersing it downstream. The resulting aggradation in-channel and over any available floodplain buries former geomorphic features creating an RA-forced disturbed landscape. The persistence and distinctiveness of this disturbance and subsequent fluvial recovery is currently poorly quantified (Hancox et al., 2005; Dunning et al., 2006; Hewitt, 2006; Korup and Clague, 2009; Korup et al., 2010).

Landslide and lake-derived fill and the associated boulder lag deposit (e.g., the carapace), inhibit fluvial incision into bedrock (Hewitt, 2006; Ouimet et al., 2007; Korup et al., 2010) until the river has removed the debris to reach its former bed. Incision therefore lags behind the rates in rivers undisturbed by RADs. Fluvial incision rates through bedrock are important for long-term landscape evolution, as they are assumed to control the rate of catchment denudation (Burbank et al., 1996; Kirchner et al., 2001; Snyder et al., 2000; Korup et al., 2009, 2010). If RAs disturb a large number of catchments, their time scales of disruption to the fluvial system are an unknown factor in understanding landscape evolution of active orogens.

River long profiles have shown promise in identifying catchments with an RAD signal (Korup, 2006). An RAD, if it persists through either retaining a lake or as a post-outburst flood remnant can form a knickpoint, or convex step, in the normally concave river long profile (Korup, 2006) — similar to a fault displacement. This displaces the fluvial profile vertically above the original channel bed, increasing overall profile steepness and decreasing overall profile concavity (Korup, 2006), which is often distinctive in long profile data.

The RA-forced disturbances act over multiple time scales, from short-term ($<10^1$ years) localised in-channel responses; ~ $10^4$ timescale changes to erosion and deposition patterns in a catchment (Whipple, 2004; Davies and Korup, 2007; Hewitt et al., 2008; Korup et al., 2009) and, potentially geologic timescales as bedrock river profiles adjust to a blockage (Korup, 2006). Some channels may never 'recover' from the interruption, and will adjust to a new RAD or RAD remnant controlled form of equilibrium, whilst other parts of the system, such as alluvial fans, may exhibit cyclic patterns of behaviour controlled by repeated upstream RAD inputs (Davies and Korup, 2007).

Concavity and steepness indices of river profiles have been used as geomorphic indicators (Korup, 2006) to distinguish between the complex interacting tectonic, lithological, and climatic drivers and more localised RA-forced deviations in long profiles using known RA locations. Steepness and concavity indices are based on Flint's Law (Flint, 1974), which describes the change of channel slope as a function of drainage area over the bedrock fluvial section of a channel, omitting alluvial and colluvial reaches in the headwaters (usually between $10^4$ and $10^6$ $m^2$, (Snyder et al., 2000; Burbank and Anderson, 2012) where debris flow processes dominate (Montgomery, 2001). Extreme local concavities (>1) are indicative of abrupt knickpoints — idealised in Fig. 1, representing transitions from incisional to depositional states — and/or strong variations in rates of tectonic uplift (Whipple, 2004).

Steep mountainous terrain can prove inaccessible or inconvenient to collect field survey data; especially for regional analyses, it is practical to extract the stream profile data from a digital elevation model (DEM). However, many regional/national DEMs may not be able to resolve comparatively small RA-forced geomorphic impacts because of their coarse resolution relative to the scales of disturbance. The DEMs are also infrequently updated, leading to only snapshots of disturbance; but if sufficient confidence is held in the quality of a DEM, it is possible to carry out field surveys for post-DEM comparison (Snyder et al., 2000), an approach we use here. This study explores the dispersion of sediment from an RAD in Ram Creek, a feeder catchment of the Buller River in northwest Nelson, South Island of New Zealand. Thirty-three years after formation, the RAD failed releasing a damaging flood. We use a combination of field-survey data and DEM analysis to yield profile metrics.

## 2. Study area

The Brunner Range, located in the Buller River basin of northwest Nelson, New Zealand, reaches a maximum elevation of 1413 m asl with relative relief in the order of a few hundred metres. Ram Creek, a tributary of Dee Creek, feeds into the large Buller River at the base of the fault-bounded Brunner Range, which continues southwest to the Tasman Sea (Fig. 2). Owing to its location west of the Alpine Fault, the Brunner Range is subjected to tectonic uplift rates of ~0.5-1.0 mm $y^{-1}$ (Wellman, 1979), with average rainfall of c. 2300 mm $y^{-1}$ (Nash et al., 2008). The east-dipping Lyell Fault crosses the Ram Creek catchment trending SW - NE near the headwaters. To the east of the fault, muscovite–biotite granites crop out; whereas to the west, rocks are composed of weaker fluvial sandstone and grey-brown mudstones (Soons, 1982; Nash et al., 2008). The river is mainly gorge-confined, typical of the west coast of the South Island, but briefly opens out for several hundred metres at the Ram Creek/Dee Creek confluence before re-entering a narrow (< 10-m) gorge.

In 1968 the Lyell Fault ruptured, resulting in the M 7.1 Inangahua earthquake that triggered numerous landslides across the NW Nelson region (Adams, 1981). The largest single valley-blocking event occurred in the headwaters of Ram Creek. A 4.4 x $10^6$ $m^3$ RA with a runout of ~700 m was deposited, c. 2.8 x $10^6$ $m^3$ of which blocked the river forming a 40-m-high dam with a 550-m crest width across the valley (Nash, 2003; Nash et al., 2008). A catchment of 4.5 $km^2$ fed water and sediment into the lake that formed behind the RAD. This dam remained stable for 13 years until in 1981, after an intense rainfall event, the dam was breached (Nash et al., 2008). Overtopping flow scoured a ~ 500-m-long, >100-m-wide (at the surface), and up to 40-m-deep triangular breach channel into the dam, eroding ~1 x $10^6$ $m^3$ of dam material (Nash, 2003; Nash et al., 2008).

Nash et al. (2008) described in detail the known sequence of events after failure; a summary is given here. The outburst flood lasted several hours and showed features more in common with a hyperconcentrated flow/debris flow rather than a Newtonian water flood because of sediment entrainment. In keeping with this interpreted rheology, the flood arrived as a series of pulses/waves, with the maximum observed at Dee Creek Bridge being around 2 m high. The bridge was destroyed, and about 22 km downstream of the confluence of Dee Creek with the Buller River a flood with a peak discharge of 4335 $m^3 s^{-1}$ was recorded 4 hours after the initial outburst event, of which 1000 $m^3 s^{-1}$ is estimated to represent the peak discharge from the dam site — 01 times the normal annual flood in Ram Creek. Flood sediment was deposited up to c. 5.5 km downstream of the breached dam. Farmland between the Ram Gorge exit and Dee Creek bridge was buried up to 2 m deep in places with sand, gravel, and large woody debris. However, most sediment deposition occurred directly below the breached dam (Nash, 2003).

## 3. Methods

### *3.1. Field survey*

Field survey data of the Ram Creek thalweg, the partially reworked outburst flood surfaces, and 15 cross sections were obtained in 2009 using an automatic total station. Survey data cover the lower extent of the RAD to the confluence with the Buller River (Fig. 3).

Clast analyses were carried out at five sites (three in Ram Creek, one in upper Dee Creek as a control, and one in lower Dee Creek) to gauge the prevalence of granitic RA sediment in the system (Figure 3). The RAD is the primary source of angular granitic rocks downstream, and the initial flooding is inferred to have deposited most sediment, with a low degree of flood-induced rounding around 5.5 km from the RAD — which is the open area at the confluence of Ram and Dee creeks.

### *3.2. River-profile extraction*

Longitudinal profiles of Ram Creek and four control streams (Dee, Rough, Brown, and Coal creeks) along the Brunner Range without RADs, but with similar climatic and tectonic histories (all cut by the Lyell Fault), were extracted from three DEMs of 100, 25, and 15 m resolution. Having a 15-m DEM for mountainous terrain is reasonably rare, hence we assess the ability of coarser data to resolve RA induced impacts. The DEMs are all based on digitised 20-m contour line data from the Land Information New Zealand (LINZ) 1:50,000 map that have then been interpolated into a DEM; the original contour lines have ± 10 m elevation error (Columbus et al., 2011). Columbus et al. (2011) compared the available DEMs and found that the 15-m DEM, which was created using a two-dimensional thin plate smoothing spline, to be the most accurate topographic data set with the least amount of artefacts in the interpolated DEM. All the available DEMs derive from the same source data; the increased quality, at a 5-m higher spatial resolution, is a result of how the source data are interpolated.

The DEM stream profiles were extracted by running hydrologically-filled DEMs in MATLAB to extract profile concavity ($\Theta$) and normalised steepness ($k_{sn}$) indices using linear regression of the log-log slope area plot. An arbitrary reference concavity ($\Theta_{ref}$) of 0.45, often used as being representative of mountainous streams (Korup, 2006), was used to normalise the steepness ($k_s$) values to allow comparisons between stream profiles. The DEMs were interpolated with 10-m contours, to ensure an even spread of data (Snyder et al., 2000; Korup, 2006; Whipple, 2004) with datum used at every height interval to avoid bias toward long flat sections when distance intervals are used (Duvall et al., 2004). A three-cell moving average was then applied to smooth each profile. Regressions over whole profile extents including colluvial and alluvial zones were also calculated (after Korup, 2006) to be used as a comparative tool to quantify forced disturbances to $k_{sn}$ and $\Theta$ indices. A forced $\Theta_{ref}$ of 0.45 was applied to the Ram Creek field survey data for direct comparison to the DEM extracted profiles using

$$k_{sn} = k_s \left(A_{cent}^{-(\Theta ref-\Theta)}\right) \qquad (2)$$

where $A_{cent}$ is the upstream catchment area of the mid-point of the studied reach (Gonga-Saholiariliva et al., 2011; Burbank and Anderson, 2012).

## 4. Results

### *4.1. Field survey*

Internal exposures of the RAD in the breach channel shows the emplaced RA dam was composed of poorly sorted, angular to subangular, <1 mm – 1 m particle sizes in a fine-grained matrix. Ram Creek has not yet cut back to the pre-landslide valley floor more than 30 years after dam failure.

The majority of the ~1 x $10^6$ $m^3$ that was eroded from the RA dam in the form of a breach channel and lake sediments were deposited directly downstream of the dam. High rates of erosion during the outburst flood produced paired terraces through the RAD showing three main stages of incision. During dam breach, the initial flood wave scoured a wide (~ 150-m) channel through the downvalley portion of the RAD to a maximum depth of 40 m at the highest point of the dam. The terracing within the RAD indicates that the flood flow narrowed downstream, to ~50 m at the distal end of the deposit. The resulting channel through the RAD has an average slope of 0.082, compared to a slope of 0.032 downstream where the river enters the narrow (~ 20–30 m) upper gorge (cross sections 10 and 11, Fig. 3). Small

(<50-cm) unpaired fill-cut adjustment terraces (Bull, 2008) and numerous abandoned channels dominate within the current valley floor, through the RA runout zone, and throughout the debris fill downstream in the upper gorge and farmland section at the Ram and Dee confluence (valley floor widths ~150 m, average slope 0.018) where the river re-enters the lower gorge. The river appears unable to remove material from the dam-break or any super-imposed material derived from the dam and lake in subsequent floods. Localised reworking seems to dominate with a number of remnant higher level surfaces that we interpret to represent the original dam-breach flood / debris flow suggesting low levels of incision. In the lower gorge the river fills the full width with little lateral accommodation space (gorge width ~ 10–20 m, average slope 0.011) for sediment storage; evidence is abundant of various ages of lateral river erosion into the bedrock gorge walls.

Very angular to subangular (Powers, 1953) granitic sediment consistent with that of the RA are found from the RAD to the Dee Creek/Ram Creek confluence (sites b, d, & e, Fig. 3). Lesser amounts of granitic sediment are found where the river re-enters the gorge downstream of the Dee Creek/Ram Creek confluence (site a, Fig. 3) to the confluence with the Buller River. The sediment mixture at the confluence is similar to that sampled in the non-RAD–affected upstream portion of Dee Creek, which has the largest proportion of subrounded to well-rounded clasts (site c, Fig. 3). The granite clasts at these non-RAD-impacted sites are far larger, likely as they were not subjected to the intense levels of fragmentation common to rock avalanche deposits and show fluvial rounding and signs of weathering. The RAD-derived sediment is dominant above the Dee Creek confluence and is overlying the pre-RA valley floor down the length of the profile — the previous valley floor is yet to be reached.

Plots of the percentage of angular and very angular clasts (termed RA), against the C40 index (short / long axis measurement) have been shown to distinguish between glacigenic facies (Benn and Ballantyne, 1994). Here, the RA-C40 plot (Fig. 4) separates the Ram Creek from the Dee Creek sediment. In sample sizes of 100 clasts we see no angular or very angular particles below the confluence, nor in the Dee Creek itself before the confluence. At the Ram:Dee confluence, we see some (granitic) angular and very angular clasts; and the upper gorge area, in the current and in the formerly occupied channel, has a higher percentage. The median diameter of clasts sampled increases downstream away from the RAD (13 mm) to 34 mm at the confluence and 49 mm in the lower Dee gorge — suggesting that it is not rounding and fining of the clasts removing the angular component.

Evidence of widening of the active channel area is found in both the upper Ram and lower Dee gorges (Figure 5). The outburst flood debris fill has vertically displaced the river bed above the pre-RA level as shown by dead tree stumps protruding from the fill marking the previous tree cover and narrower channel extent. Lateral erosional features are cut into the weak fluvial sandstone and mudstone, most commonly as gorge wall undercutting with resulting landslides / wall failure. Other features include potholes scoured into the gorge walls with a shallow covering of granitic RA debris, and joints in the mudstone which have been hydraulically wedged and widened with pebbles of more resistant lithologies. The age of these potholes are unknown, they may reflect reuse of erosional features from previous, higher, river bed levels.

### *4.2. Ram Creek profile*

The topographic 20-m contour data on which the three Ram Creek DEMs are based were updated after the RA event to incorporate the landslide-dammed lake. The presence of the RA-impounded lake in these data, which has not been present for almost 30 years, is evidenced in each DEM by a distinct flattening in the stream profile at the same elevation as the dam crest (Fig. 1). The contour data have not been updated since the 1981 outburst flood and do not reflect flood-induced changes or subsequent recovery, whereas the 2009 field data represent the intervening post-flood reworking.

The 25- and 100-m DEMs are unable to resolve the gorge as the cell size is similar to the observed gorge widths. The tops of the gorge walls (8–10 m) and higher valley floors are contained within a cell, or pair of cells. The interpolation algorithm then applied at these scales smooths between these cells resulting in the loss of sharp gorge walls and underestimating the depth of the gorge. As a result these DEMs consistently report channel-profile elevations higher than the 15-m DEM and field profile (Figure 6). The interpolation method used to create the 15-m DEM specifically maintains sharp edges (Columbus et al., 2011), which are appropriate for this locality.

The 2009 field survey profile closely follows the 15-m DEM profile for much of the course (Fig. 6). The 25- and 100-m profiles deviate substantially from the field survey but capture the general shape to within ± 10–15 m vertically. For much of the profile, the cell size of the 25- and 100-m DEMs exceed the alluvial valley width as measured in the field. The majority of the field survey remains slightly below the three DEM profile elevations, but there are significant differences at the confluence with the Buller River and 4.5–5 km upstream of the confluence (where the river flows into the narrow upper gorge). These reaches have field-measured profiles *c*. 6 to 15 m lower than the 15-m DEM.

Table 1 shows the $\Theta$ and $k_{sn}$ indices for Ram Creek derived from DEMs and field surveying. The DEMs (fluvial only profiles) are cropped to the field survey extent presented in the Log A–Log S plot in Figure 6. The 25 m and 100 m DEM profiles have broadly similar normalised steepness indices, however both are a significant over-estimation in concavity in comparison to the 15 m DEM.

When comparing the field data to the 1981 RAD-impacted 15-m DEM, the data show that the profile 30 years after the outburst flood has reduced by c. 0.079 (-7%) in its concavity and steepened by c. 3.34 (7%). This is attributed to the immediate post-flood aggradation and the continued (slow) downstream dispersion of the RAD, as predicted by Nash et al. (2008 p. 192) and described in the field evidence section above.

***4.3. Normalised steepness and concavity indices of the Brunner streams***

The 'true' profiles of Dee, Rough, upper Brown and Coal creeks are unknown. Here, using the gross similarity of the 15-m DEM Ram Creek profile with the field survey and the work of Columbus et al. (2011) we assume the 15-m DEM to give the most accurate river profile. This allows us to evaluate the ability of DEM metrics to identify an RAD presence. No known RA events have impacted on the surrounding streams in recent times. Regressions over whole profiles (including colluvial, bedrock fluvial, and alluvial sections) as well as fluvial-only reaches are presented in Table 1. Whole profiles produce higher variations in metrics between each of the stream profiles. However, the 100-m DEM is always steeper, and of higher concavity than the 25- and 15-m DEMs — this is consistent with the pattern shown for Ram Creek and is likely related to the simplification of the narrow, steep, and gorge-confined fluvial topography and will not be discussed further.

The 15-m DEM $\Theta$ of the Brunner streams are not statistically different using the whole profile, unlike their $k_{sn}$. Ram Creek, Brown Creek, and Rough Creek share similar whole profile $k_{sn}$, whilst Dee Creek (of which Ram is a tributary) and Coal Creek are much less steep. On this basis, nothing distinguishes Ram Creek as being different, i.e., having an RAD deposit perturbing the DEM profile metrics.

The comparison of the 15-m long profiles and slope–area plots (Figs. 1 and 6) show, apart from Dee and Ram creeks, extremely prominent knickpoints in the bedrock fluvial slope–area domain. Profile metrics have been calculated either side of these knickpoints (Table 1). The $\Theta$ and $k_{sn}$ increase from the upstream sections to the downstream sections. Concavities increase by an average of 44%, whilst steepness increases on average by 103%. This masks significant spatial trends: downstream reaches get less steep moving north, whilst upstream reaches get steeper, and the absolute difference in upstream–downstream $k_{sn}$ values decreases. By Rough Creek we see little difference in $k_{sn}$ either side of the knickpoint and. as described, no discernible knickpoints in Ram and Dee creeks. In Ram, the visually obvious RA knickpoint (Fig. 7) is deemed to be part of the 'colluvial' domain using the standard methodologies outlined.

## 5. Discussion

### *5.1. Field evidence*

Averaged incision rates through the reworked granitic RA debris for the highest and lowest terraces relative to the current river are at maximum ~160 mm $y^{-1}$ (cross section 4) since dam failure and a minimum ~ 25 mm $yr^{-1}$ (cross section 10) since the outburst flood. This is an order of magnitude larger than the estimated fluvial incision rates of the Westland rivers cutting across the Alpine Fault, around 10 mm $y^{-1}$, broadly in equilibrium with tectonic uplift (Tippett and Kamp, 1995). However, the high terraces are likely to be a product of the outburst flood itself and not of fluvial (re)incision since 1981 based on an observed lack of reworking and features consistent with a debris flow / high sediment concentration flood. Small (<50-cm), unpaired, fill-cut adjustment terraces (Bull, 2008) and abandoned channels throughout the length of the profile, however, indicate internal adjustment, instability, and lateral reworking of the dispersed RA debris and are interpreted to reflect the past 30 years of geomorphic adjustment. This has failed to incise back to the previous valley floor, let alone keep pace with likely uplift rates (in the order of a few mm $y^{-1}$).

In pre-RA Ram Creek and in the other Brunner streams (including the far larger Buller River) vertical erosion is thought to dominate based on the narrow bedrock gorge topography. Ram Creek is anomalous; in locations where other streams are highly confined and single channel, it has a wider active multithread channel area with abundant stored sediment.

The outburst-flood influx of RA sediment has ensured that the channel is transport-limited, and the channel has not been able to recover fully in the last 30 years. The fill of RA sediment covering the bedrock floor (Fig. 5B) throughout the profile has vertically displaced Ram Creek as evidenced in the DEM analysis. The granitic RA debris is acting as a 'cover' preventing post-outburst flood vertical incision of the pre-RA weak sedimentary bedrock floor rather than as abrasive 'tools' to promote erosion. The RA-C40 (Fig. 4) suggests the fines that comprise the bulk of the RAD are still dispersing and have not migrated past the Ram:Dee confluence. This is in contrast to the immediate dispersion of a large amount of dam and lake sediment in the initial outburst flood. The result has been lateral channel switching in response to localised aggradation and reworking. Where this has brought the channel into contact with the weak sedimentary gorge walls, lateral bevelling (Fig. 5C-D) is evident. This is far easier for the 'normal' Ram Creek flood flows to erode the gorge walls, when locally redistributing the far more resistant RA granitic debris, than to incise the covered bed. This is conceptually similar to the formation of 'epigenetic gorges' in the work of Hewitt (1998). If this situation persists, gorge widening through undercutting is likely to occur, with evidence of this in the form of undercut gorge walls, fallen blocks and what we interpret to be toe-erosion–driven gorge-wall failure occurring (Fig. 5E). This has been conceptualised in the 'fill and bevel' model of Hancock and Anderson (2002) of bedrock strath formation, whereby a valley fill (in their case climatically driven) protects the valley floor whilst lateral bevelling takes place. This requires a far smaller volume of rock to be eroded during strath formation as opposed to those driven by a period of quiescence in tectonic uplift. This erosive bevelling is unrelated to tectonics or climate — it is driven by landslide dam-driven aggradation resulting from sediment dispersion.

There are notable deviations from this situation; one is in the gorge downstream of the Ram/Dee Creek confluence, especially near the confluence with the far larger Buller River. In the 1-km reach until the confluence, a knickpoint is clear with field data elevations below the 15 m DEM, with little field evidence of RAD sediment. However, if this has only occurred since the pre-RAD DEM, it suggests unrealistically high rates of bedrock incision — a maximum of 460 mm $y^{-1}$. We interpret difference to reflect a number of factors; outburst flood flushing of existing bedload, as most debris was trapped upstream of this section of gorge leaving a more water-rich, sediment-poor flood to pass this point; continued background incision as the stream attempts to keep pace with uplift, and grade to the more powerful Buller River incision; and, finally, poor DEM coverage in what is the narrowest part of the gorge system. The other valid possibility is that this results from a number of previous episodes similar to the 1968 RA that have delivered high volumes of buffering bedload to the upper system, whilst the lower sections remain able to use their more limited cover as erosional tools. The other notable deviation in the field to DEM data is the field-measured incision where Ram Creek gorge widens (c on Fig. 6). This is a zone of flow expansion and outburst flood deposition in the form of a fan of sediment. We interpret the subsequent drop in river thalweg at this point to reflect localised post-flood entrenchment into this fan (cross section 13), with the pre-flood valley floor not yet reached. This is analogous to the modelling and field data presented by Davies and Korup (2007) for a far larger gorge-exit location where the Poerua River emanating from a narrow gorge has become deeply entrenched into an alluvial fan whose recent aggradation was driven by an RAD breach.

Over 30 years since dam failure, ~3.4 x $10^6$ $m^3$ of the original RAD still remains, including boulders from the carapace not eroded by the outburst flood or subsequent dispersion stored in the headwaters. The lag deposit forms a minor knickpoint. The remnant RAD is sporadically inputting debris into Ram Creek, although we interpret most reworking is local. Thus, Ram Creek could potentially remain disturbed over long time scales, up to $10^4$ years based on work in other catchments (Davies and Korup, 2007; Korup et al., 2009). To return the river to true equilibrium with uplift and incision by the Buller River will require ~6 km of progression of the knickpoint near the Buller River to steepen the profile enough to transport the RAD sediments. Alternatively, a further rupture on the Lyell Fault may steepen the profile sufficiently, but at the same time will induce seismic landslides adding additional cover to the channel. In the timescales of recovery posed here, the system likely will be interrupted by another large landslide, equilibrium is unlikely to ever be attained in this catchment.

### *5.2. Brunner stream profiles*

The significant changes in profile metrics in the Brunner streams (Ram included) may be related to either differential movement on the Lyell Fault (which becomes unmapped near Rough Creek) or to changing lithology. Coal, Brown, and Rough creeks all cut through a unit of metasedimentary rocks after the initial headwater granite intrusion before reaching the sedimentary rocks, while Dee and Ram creeks pass directly from granites to the sedimentary rocks.

Such prominent knickpoints related to tectonics and lithological variations make the recognition of minor RAD knickpoints (low percentage change in metrics) extremely difficult without other evidence, and so restricts the possibility of automated extraction of likely RAD positions in DEMs based on within-region variation, even with high-resolution DEMs.

Having the evidence and observational data, and a pre- and post-flood profile, has allowed the tentative quantification of change to profile metrics through time. Korup (2006) stated that removing a RAD from a long profile on average increases concavity by 1% and reduces steepness by 10%. Following this, and by using the 15-m DEM for the intact dam and the field profile as a snapshot of the dispersing dam, a tentative recovery envelope of the Ram Creek long profile back to pre-RA indices has been idealised in Fig. 8. The speed of fluvial profile recovery is dependent upon the rate at which Ram Creek can remove the RAD debris fill down the length of the long profile into the Buller River and incise back to pre-RA channel bed elevations.

Using Dee Creek as a control (comparable rainfall, elevation, geology, but no knickpoint), Table 1 shows that the RAD has decreased the normalised steepness and increased concavity indices of the Ram Creek fluvial profile (assuming the pre-RA Ram Creek profile did not contain a knickpoint). The reverse pattern is shown by the whole profile indices.

## 6. Conclusion

The 1968 Ram Creek RA has resulted in major geomorphic disturbance, firstly, through emplacement and blockage of Ram Creek, and secondly, as a result of the outburst flood. Much geomorphic work was achieved by the outburst flood shown by 40 m of incision into the RA dam crest and by transportation of a proportion of the eroded RA debris out of the catchment to the Buller River. However, channel aggradation of RA debris > 5 km downstream of the RAD indicates that a large proportion of the material eroded from the RAD is still being stored within the catchment. The RA-forced disturbances to Ram Creek have since been dispersed over a larger area than the initial deposit. The continued chronically disturbed state of Ram Creek contradicts the behaviour of the rivers in the Southern Alps, New Zealand, which are thought to be underloaded and to transport all of the sediment (including landslide sediment) that is supplied to them (Burbank and Anderson, 2012). The RA outburst flood fill acts as a buffer providing a cover effect over the pre-RA topography, but it is also a source of granitic tools used to laterally erode the weak bedrock gorge walls, resulting in secondary landsliding along the length of the profile by undercutting. Over longer temporal scales, the outburst flood alluvial fill along Ram Creek could create a RA-forced strath terrace under the sediment loading model (Hancock and Anderson, 2002), as the stream bevels bedrock walls faster than it incises the dispersed landslide fill. An RA-forced strath terrace would last long after evidence of the original deposit has been eroded, but has no tectonic significance in the normal sense of what a strath is though to represent, there was no period of tectonic quiescence to allow lateral bevelling. The only tectonic significance is that a fault rupture triggered the RAD, and in larger ruptures there may be a regional signature to RAD interruptions; however, many RAs are triggered by nonseismic events.

The complete removal of stored landslide debris may extend over long temporal scales, possibly ~$10^4$ years as suggested by Korup et al. (2009). This questions the importance of the cover effect on the long-term bedrock incision rates in Ram Creek and has implications for landscape evolution (Whipple, 2004; Ouimet et al., 2007; Lague, 2010). In regions as active as New Zealand the time scales of recovery are significantly longer than the recurrence interval of earthquakes likely to generate large landslides that would disrupt Ram

Creek again. This suggests a permanently disturbed landscape that will not attain equilibrium, a situation that might be similar to many other catchments.

The $\Theta$ and $k_{sn}$ Concavity indices derived from field and DEM data show that the RAD-induced knickpoint has less of an impact on profile metrics than knickpoints caused by differential uplift rates and lithologies with varying resistance to erosion. This makes automated recognition of landslide-interrupted river systems exceptionally difficult; hence we suggest that they are underrepresented.

**Acknowledgements**

Fieldwork was in part supported by a small grant from the Royal Geographical Society (SD), which we gratefully acknowledge. We thank three anonymous reviewers for their suggestions and comments. We would like to acknowledge the efforts and patience of Richard Marston in correcting our abuse of language and grammar in earlier drafts.

**References**

Adams, J. 1980. Contemporary uplift and erosion of the Southern Alps, New Zealand: Summary. Geological Society of America Bulletin, Part 1, 91, 2-4.

Adams, J. 1981. Earthquake-dammed lakes in New Zealand. Geology 9, pp. 215-219.

Benn, D. I. and Ballantyne, C. K. 1994. Reconstructing the transport history of glacigenic sediments: a new approach based on the co-variance of clast form indices. Sedimentary Geology 91, 215-227.

Bull, W. B. 2008. Tectonic geomorphology of mountains: A new approach to paleoseismology. Blackwell Publishing Ltd, Oxford, UK.

Burbank, D. W. and Anderson, R. S. 2012. Tectonic Geomorphology ,Second Edition. Wiley-Blackwell Publishing, Chichester, UK.

Burbank, D. W., Leland, J., Fielding, E., Anderson, R. S., Brozovic, N., Reid, M. R., and Duncan, C. 1996. Bedrock incision, rock uplift and threshold hillslopes in the northwestern Himilayas. Nature 379, 505-510.

Columbus, J., Sirguey, P., and Tenzer, R. 2011. A free fully assessed 15 metre digital elevation model for New Zealand. Survey Quarterly 66, 16-19.

Costa, J. E., and Schuster, R. L. 1988. The formation and failure of natural dams. Geological Society of America Bulletin 100, pp. 1054-1068.

Davies, T. R. H., and Korup, O. 2007. Persistent alluvial fanhead trenching resulting from large, infrequent sediment inouts. Earth Surface Processes and Landforms 32, 725-742.

Davies, T, R. H,, McSaveney, M. J., and Hodgson, K. A. 1999. A fragmentation-spreading model for long-runout rock avalanches. Canadian Geotechnical Journal 36, 1096-1110.

Dunning, S. A., Petley, D. N., Rosser, N. J., and Strom, A. L. 2005. The morphology and sedimentology of valley confined rock-avalanche deposits and their effect on potential dam hazard. In: Hungr, O., Fell, R., Couture, R., and Eberhardt, E. (Eds.), Landslide Risk Management. Taylor and Francis Group, London, pp 691-701.

Dunning, S. A., Rosser, N. J., Petley, D. N., and Massey, C. R. 2006. Formation and failure of the Tsatichhu landslide dam, Bhutan. Landslides 3, 107-113.

Duvall, A., Kirby, E., and Burbank, D. 2004. Tectonic and lithologic controls on bedrock channel profiles and processes in coastal California. Journal of Geophysical Research 109, pp18.

Flint, J. J. 1974. Stream gradient as a function of order, magnitude, and discharge. Water Resources research 10 (5), 969-973.

Gonga-Saholiariliva, N., Gunnell, Y., Harbor, D., and Mering, C. 2011. An automated method for producing synoptic regional maps of river gradient variation: Proceedure, accuracy tests, and comparison with other knickpoint mapping methods. Geomorphology 134, 394-407.

Hancock, G, S., and Anderson, R. S. .2002. Numerical modelling of fluvial strath terrace formation in response to oscillating climate. GSA Bulletin 114 (9), 1131-1142.

Hancox, G. T., McSaveney, M. J., Manville, V. R., and Davies, T. R. 2005. The October 1999 Mt Adams rock avalanche and subsequent landslide dam-break flood and effects in Poerua River, Westland, New Zealand. New Zealand Journal of Geology and Geophysics 48, 683-705.

Hewitt, K. 1998. Catastrophic landslides and their effects on the Upper Indus streams, Karakoram Himalaya, northern Pakistan. Geomorphology 26, 47-80.

Hewitt, K. 1999. Quaternary moraines vs catastrophic rock avalanches in the Karakoram Himalayas, Northern Pakistan. Quaternary Research 51, 220-237.

Hewitt, K. 2006. Disturbance regime landscapes: mountain drainage systems interrupted by large rockslides. Progress in Physical Geography 30 (3), 365-393.

Hewitt, K. 2009. Catastrophic rock slope failures and late Quaternary developments in the Nanga Parbat-Haramosh Massif, Upper Indus basin, northern Pakistan. Quaternary Science Reviews 28, 1055-1069.

Hewitt, K., Clague, J. J., and Orwin, J. F. 2008. Legacies of catastrophic rock slope failures in mountain landscapes. Earth Surface Reviews 87, 1-38.

Hovius, N., Stark, C. P., and Allen, P. A. 1997. Sediment flux from a mountain belt derived by landslide mapping. Geology 25 (3), 231-234.

Kirchner, J. W., Finkel, R. C., Riebe, C. S., Granger, D. E., Clayton, J. L., King, J. G., and Megahan, W. F. 2001. Mountain erosion over 10 yr, 10 k.y., and 10 m.y. timescales. Geological Society of America 29 (7), 591-594.

Korup, O. 2005a. Geomorphic imprint of landslides on alpine river systems, southwest New Zealand. Earth Surface Processes and Landforms 30, 783-800.

Korup, O. 2005b. Distribution of landslides in southwest New Zealand. Landslides 2, 43-51.

Korup, O. 2006. Rock-slope failure and the river long profile. Geology 34 (1), 45-48.

Korup, O., and Clague, J. J. 2009. Natural hazards, extreme events and mountain topography. Quaternary Science Reviews 28, 977-990.

Korup, O., McSaveney, M. J., and Davies, T. R. H. 2004. Sediment generation and delivery from large historic landslides in the Southern Alps, New Zealand. Geomorphology 61, 189-207.

Korup, O., Densmore, A. L., and Schlunegger, F. 2009. The role of landslides in mountain range evolution. Geomorphology 120 (1-2), 77-90.

Korup, O., Montgomery, D, R, and Hewitt, K. 2010. Glacier and landslide feedbacks to topographic relief in the Himilayan syntaxes. PNAS 107 (12), 5317-5322.

Lague, D. 2010. Reduction of long-term bedrock incision efficiency by short-term alluvial cover intermittency. Journal of Geophysical Research 115, 23pp.

McSaveney, M. J. 2002. Recent rock-falls and rock avalanches in Mount Cook National Park, New Zealand, in Evans, S. G., and DeGraff, J. V. (Eds.), Catastrophic Landslides: Effects, Occurrence, and Mechanisms. Boulder, Colorado: Geological Society of America Reviews in Engineering Geology, v. XV, pp 35-70.

Mitchell, W. A., McSaveney, M. J., Zondervan, A., Kim, K., Dunning, S. A., and Taylor, P. J. 2007. The Keylong Serai rock avalanche, NW Indian Himalaya: geomorphology and Palaeoseismic implications. Landslides 4, 245-254.

Montgomery, D. R. 2001. Slope distributions, threshold hillslopes, and steady state topography. American Journal of Science 301, 432-454.

Montgomery, D. R., and Brandon, M. T. 2002. Topographic controls on erosion rates in tectonically active mountain ranges. Earth and Planetary Science Letters 201, 481-489.Nash. T. R. 2003. Engineering geological assessment of selected landslide dams formed from the 1929 Murchison and 1968 Inangahua earthquakes. M.Sc .Thesis, Engineering Geology, University of Canterbury, New Zealand.

Nash, T., Bell, D., Davies, T., and Nathan, S. 2008. Analysis of the formation and failure of Ram Creek landslide dam, South Island, New Zealand. New Zealand Journal of Geology and Geophysics 51, 187-193.

Ouimet, W. B., Whipple, K. X., Royden, L. H., Sun, Z., and Chen, Z. 2007. The influence of large landslides on river incision in a transient landscape: Eastern margin of the Tibetan Plateau (Sichuan, China). GSA Bulletin 119, 1462-1476.

Pearce, A. J., and Watson, A. J. 1986. Effects of earthquake-induced landslides on sediment budget and transport over a 50 year period. Geology 14, 52-55.

Powers, M. C. 1953. A new roundness scale for sedimentary particles. J. Sed. Petrol. 23 117-119.

Reznichenko, N, V., Davies, T. R. H., and Alexander, D. J. 2011. Effects of rock avalanches on glacier behaviour and moraine formation. Geomorphology 132, 327-338.

Snyder, N. P., Whipple, K. X., Tucker, G. E., and Merritts, D. J. 2000. Landscape response to tectonic forcing: Digital elevation model analysis of stream profiles in the Mendocino triple junction region, northern California. GSA Bulletin 112 (8), 1250-1263.

Soons, J. M. 1982. Westland: The west coast of the South Island. In: Soons, J. M., and Selby, M. J. (eds) Landforms of New Zealand. Auckland: Longman Paul, pp. 299-315.

Tippett, J. M, and Kamp, P. J. J. 1995. Quantitative relationships between uplift and relief parameters for the Southern Alps, New Zealand, as determined by fission track analysis. Earth Surface Process and Landforms 20, 153-175.

Wellman, H. W. 1979. An uplift map for the South Island of New Zealand, and a model for uplift of the Southern Alps. Royal Society of New Zealand Bulletin 18, 13-20.

Whipple, K. X. 2004. Bedrock rivers and the geomorphology of active orogens. Annual Reviews of Earth and Planet Science 32, 151-185.

Fig. 1. Conceptual model of an idealised profile (including colluvial, bedrock fluvial, and alluvial reaches) in a log slope–log area space; (A) profile without a knickpoint; (B). profile with a knickpoint. The transition from colluvially dominated to bedrock fluvial-dominated process is the same as (A). However, a knickpoint causes another break within the bedrock fluvial region by an increase in slope with increasing area, which reflects an increase in profile steepness (*ks*) in the reach below the knickpoint.

Fig. 2. Location of the streams along the Brunner Range, NW Nelson, South Island, New Zealand. From north to south: Ram Creek (field data), Dee Creek, Rough Creek, Brown Creek, and Coal Creek (DEM analyses).

Fig. 3. (A) Map showing the Dee Creek catchment and sites referred to in the text. (B) Cross section graphs showing the changing confinement of Ram Creek downstream as it passes through two bedrock gorges. (C) Cumulative distribution of sampled clast angularity tracking distribution of RA debris. Sampled clasts from the RA down to the Ram and Dee confluence have a more angular distribution (PSA sites b, d, and e) than the 'normal' Dee Creek distribution (PSA site c). In the lower Dee Creek (PSA site a), some of the angular RA signal is lost because of sediment mixing after the confluence.

Fig. 4. RA-C40 graph of clasts sampled in the Ram-Dee creeks catchment, location codes as Fig. 1. Sites below the Ram:Dee confluence show no angular component.

Fig. 5. (A). Pothole scoured into Ram Creek gorge wall filled with granitic RA debris (glasses for scale); (B). view upstream of outburst flood fill in Ram gorge, note valley floor widening shown by protruding dead trees (right); (C) lateral erosion and hydraulic wedging of the Dee Creek gorge walls (notebook for scale); (D) view downstream in Ram Gorge showing bevelling of the gorge walls (box).

Fig. 6. (upper) Vertically exaggerated Ram Creek profiles from the field survey and the three DEM extracted profiles cropped to the same extent. At 5 km from the mouth, the survey profile begins to increase in elevation above the DEM profiles. Letters delimit geomorphic zones: a, wide gorge below the RA; b, narrow bedrock gorge; c, gorge widening; d, unconfined; and e, Dee Creek bedrock gorge. (Lower) DEM regressions cropped to the extent of the field survey. Note the slight change in the slope of the regression lines, especially from the 25-m DEM profile.

Fig. 7. Slope–area plots of the Brunner streams, 15-m DEM is red, 25-m DEM is blue, and 100-m DEM is green. Greyed areas represent fluvial only (excluding colluvial and alluvial reaches) regression extents. Large knickpoints, Kp, can be seen in profiles from range-bounding faults, in Coal, Rough, and upper Brown creeks. The RA-induced knickpoint can be seen in the Ram profile, but it does not induce the same break in the log–log space as a range-bounding fault. Dee Creek is the only profile that does not contain a knickpoint.

Fig. 8 Idealised recovery envelope of the steepness and concavity of Ram Creek long profile back to pre-RA indices. 'Normal' river indices are based on Korup (2006). The speed of fluvial recovery is dependent on the erosional efficiency of Ram Creek to incise back to pre-RA channel bed elevations.

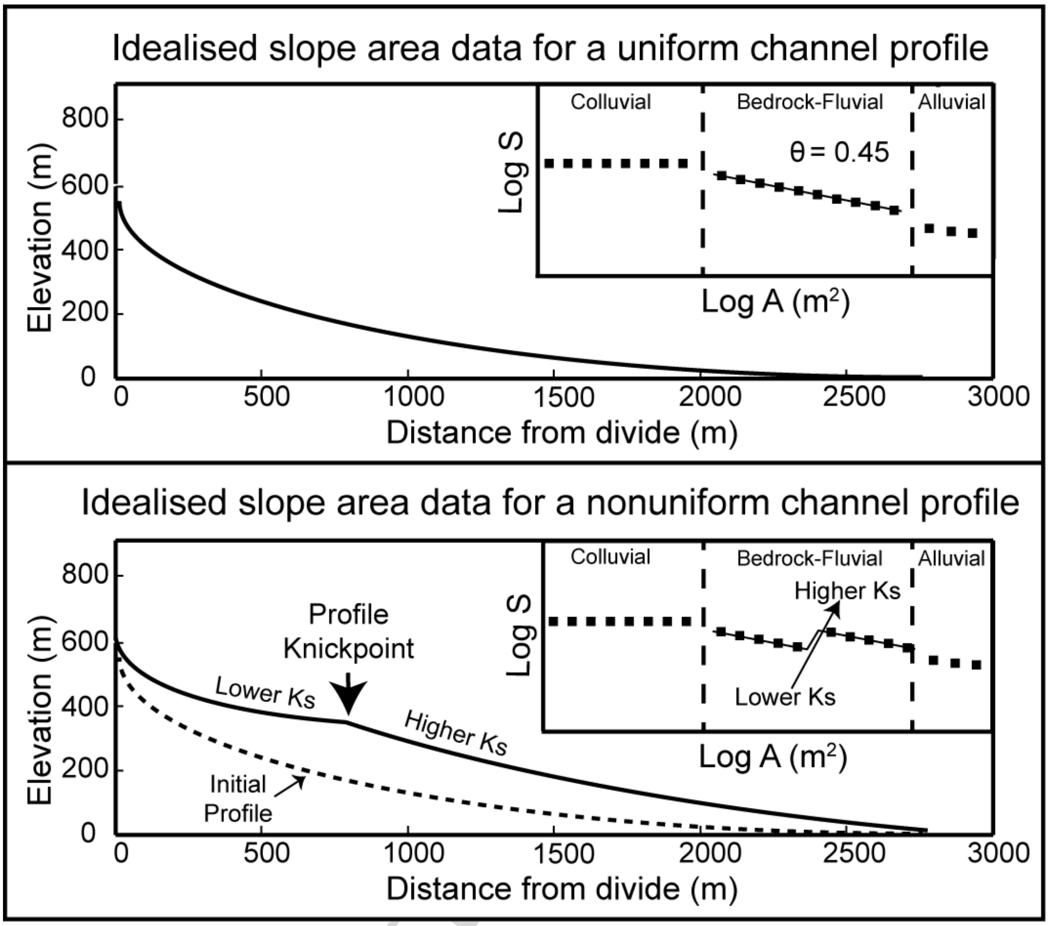
Idealised slope area data for a uniform channel profile
Elevation (m)
800
600
400
200
0
0
500
1000
1500
2000
2500
3000
Distance from divide (m)
Colluvial
Bedrock-Fluvial
Alluvial
Log S
θ = 0.45
Log A (m²)
Idealised slope area data for a nonuniform channel profile
Profile
Knickpoint
Lower Ks
Higher Ks
Initial
Profile
Higher Ks
Lower Ks

Figure 1

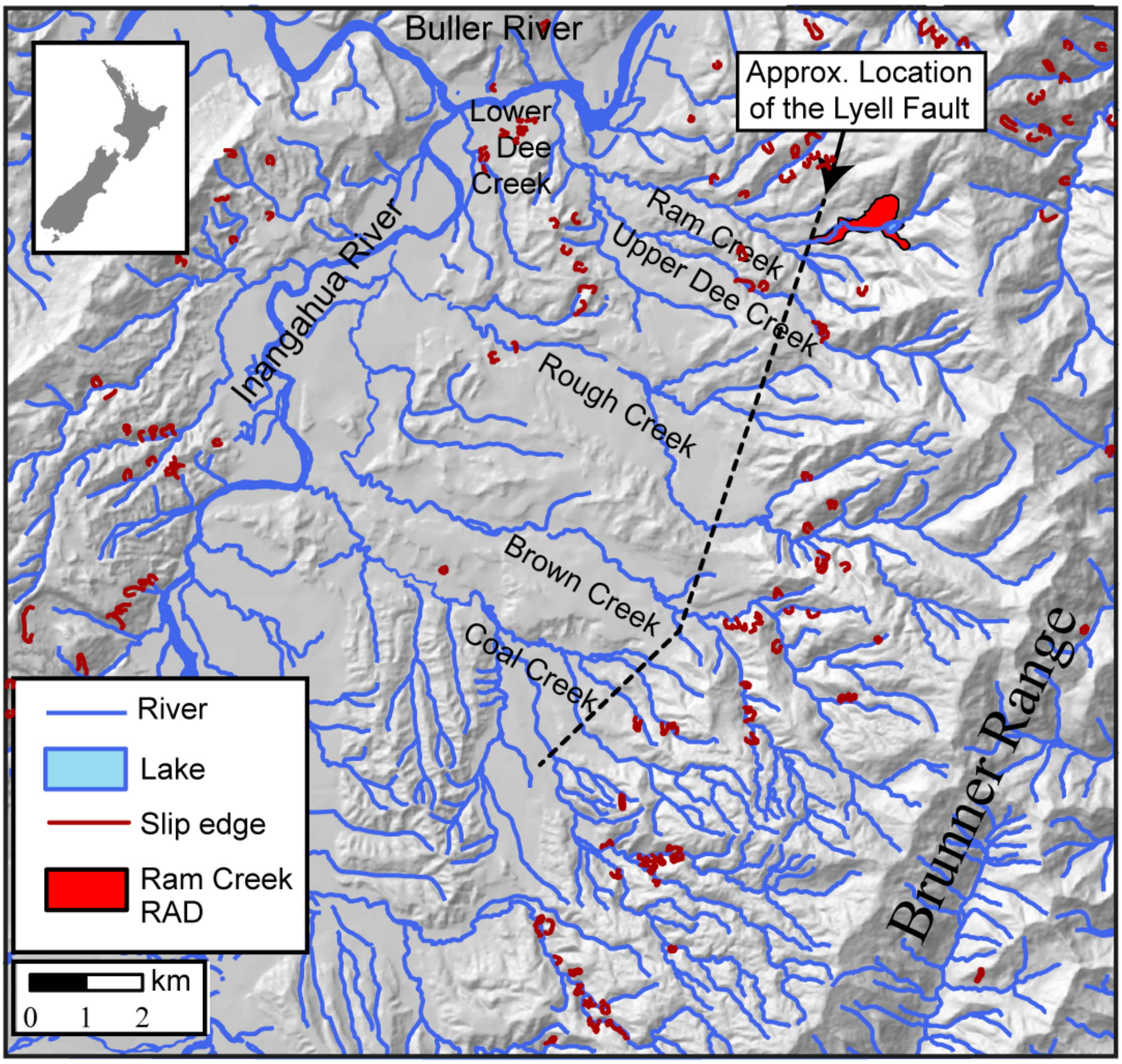

Buller River
Approx. Location of the Lyell Fault
Lower Dee Creek
Ram Creek
Upper Dee Creek
Inangahua River
Rough Creek
Brown Creek
Coal Creek
Brunner Range
River
Lake
Slip edge
Ram Creek RAD
km
0 1 2


Figure 2

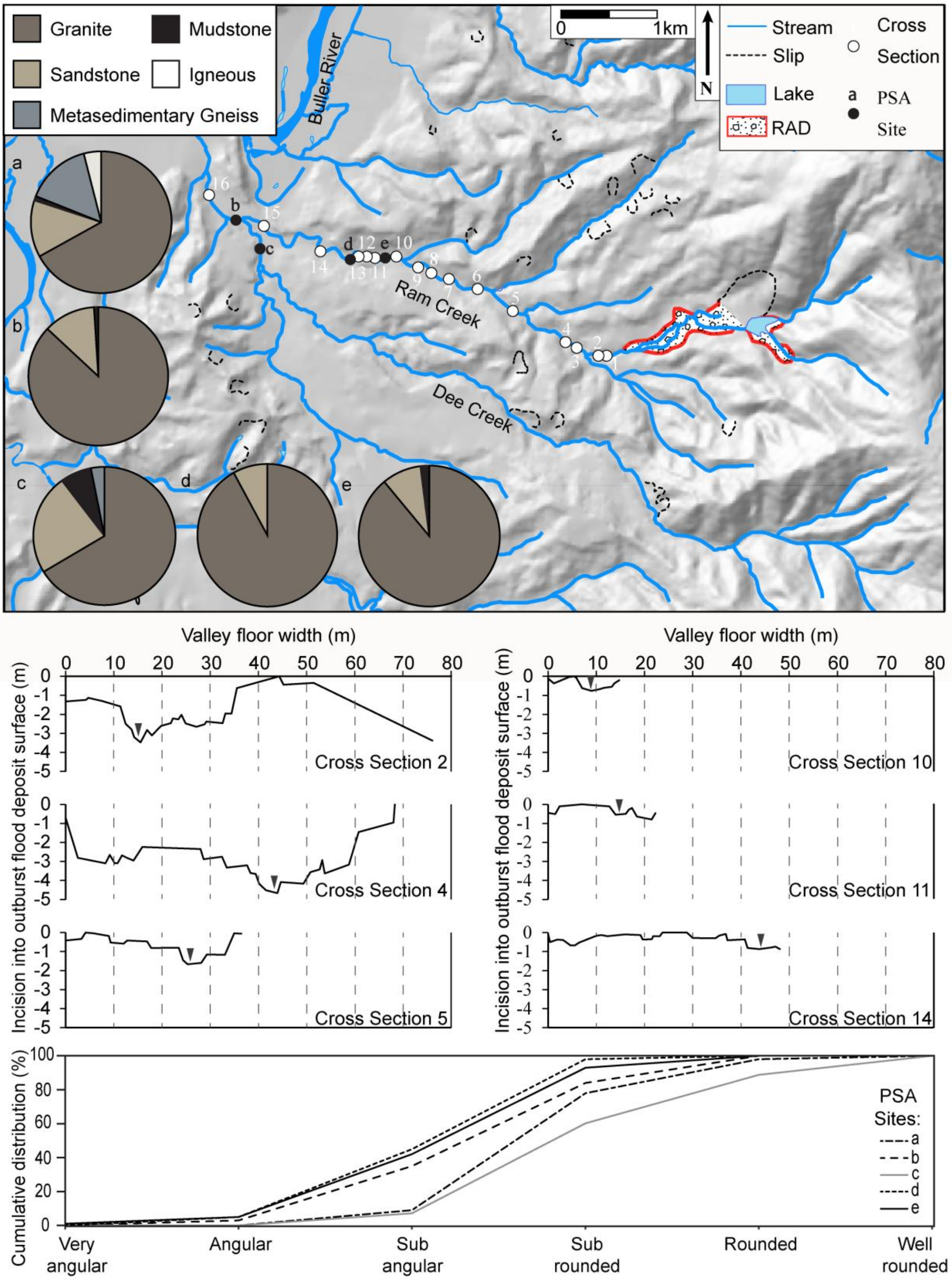

Granite
Mudstone
Sandstone
Igneous
Metasedimentary Gneiss
0
1km
N
Stream
Slip
Lake
RAD
Cross Section
a PSA Site
Buller River
Ram Creek
Dee Creek
Valley floor width (m)
Incision into outburst flood deposit surface (m)
Cross Section 2
Cross Section 4
Cross Section 5
Cross Section 10
Cross Section 11
Cross Section 14
Cumulative distribution (%)
Very angular
Angular
Sub angular
Sub rounded
Rounded
Well rounded
PSA Sites:


Figure 3

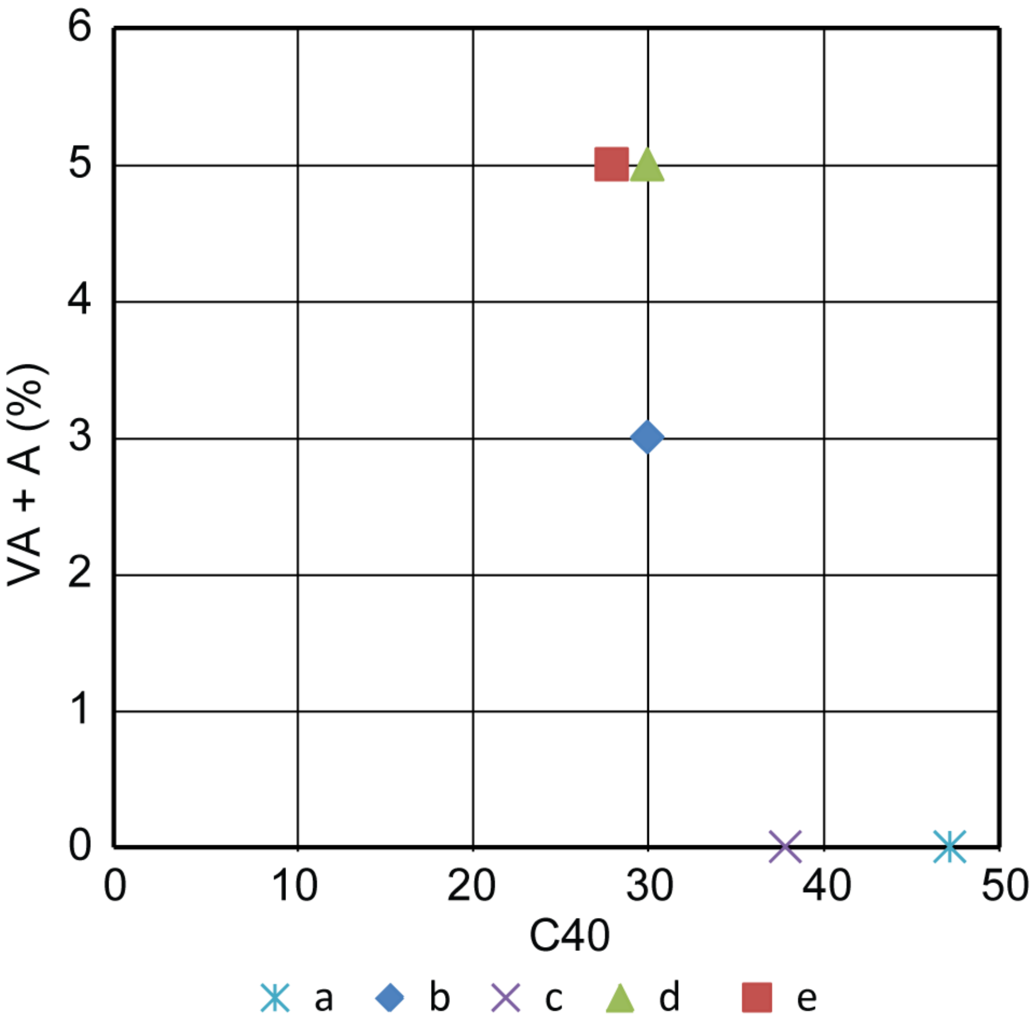


Figure 4


Figure 5

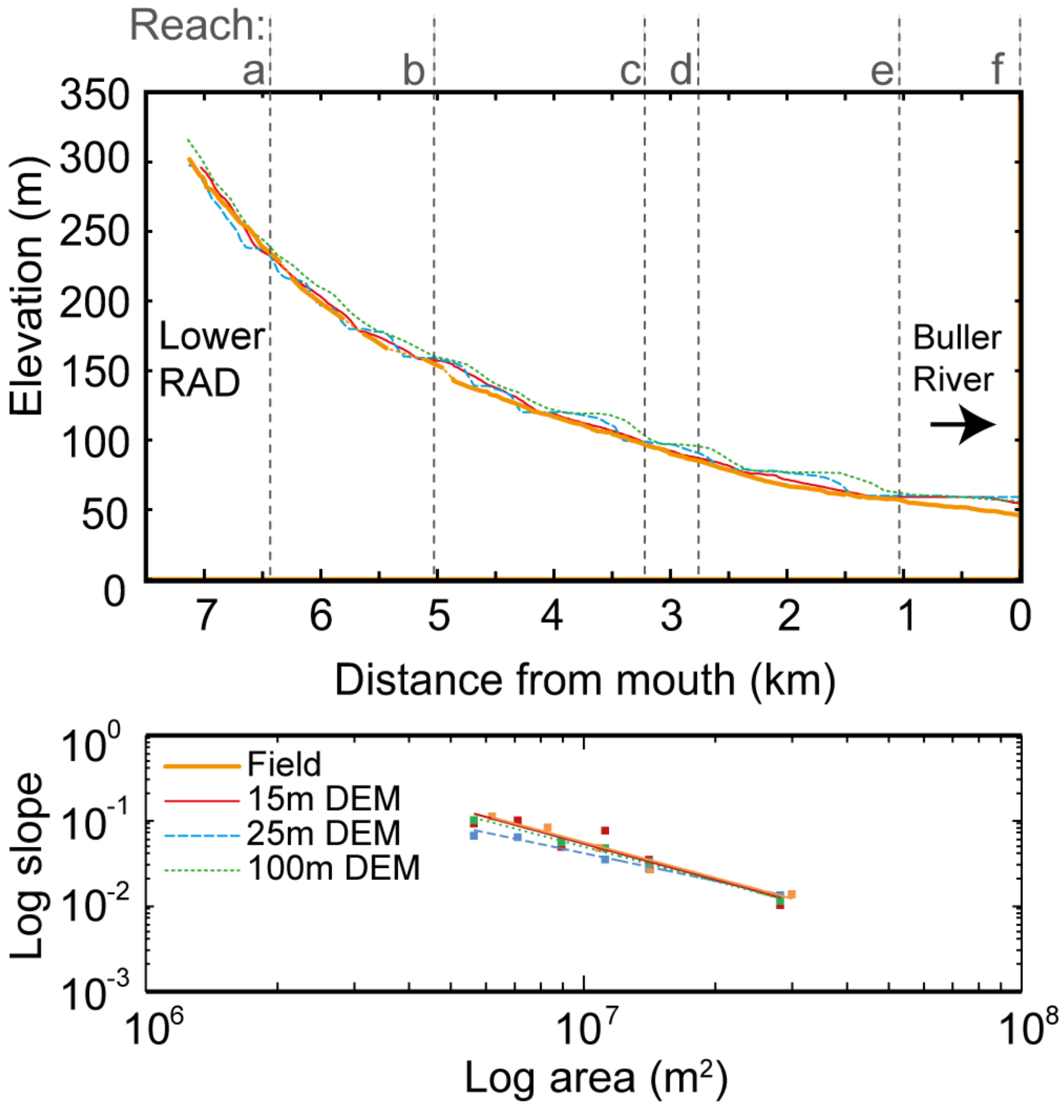
Reach:
a
b
c
d
e
f
350
300
250
200
150
100
50
0
Elevation (m)
Lower RAD
Buller River
7
6
5
4
3
2
1
0
Distance from mouth (km)
$10^0$
$10^{-1}$
$10^{-2}$
$10^{-3}$
Log slope
Field
15m DEM
25m DEM
100m DEM
$10^6$
$10^7$
$10^8$
Log area ($m^2$)

Figure 6

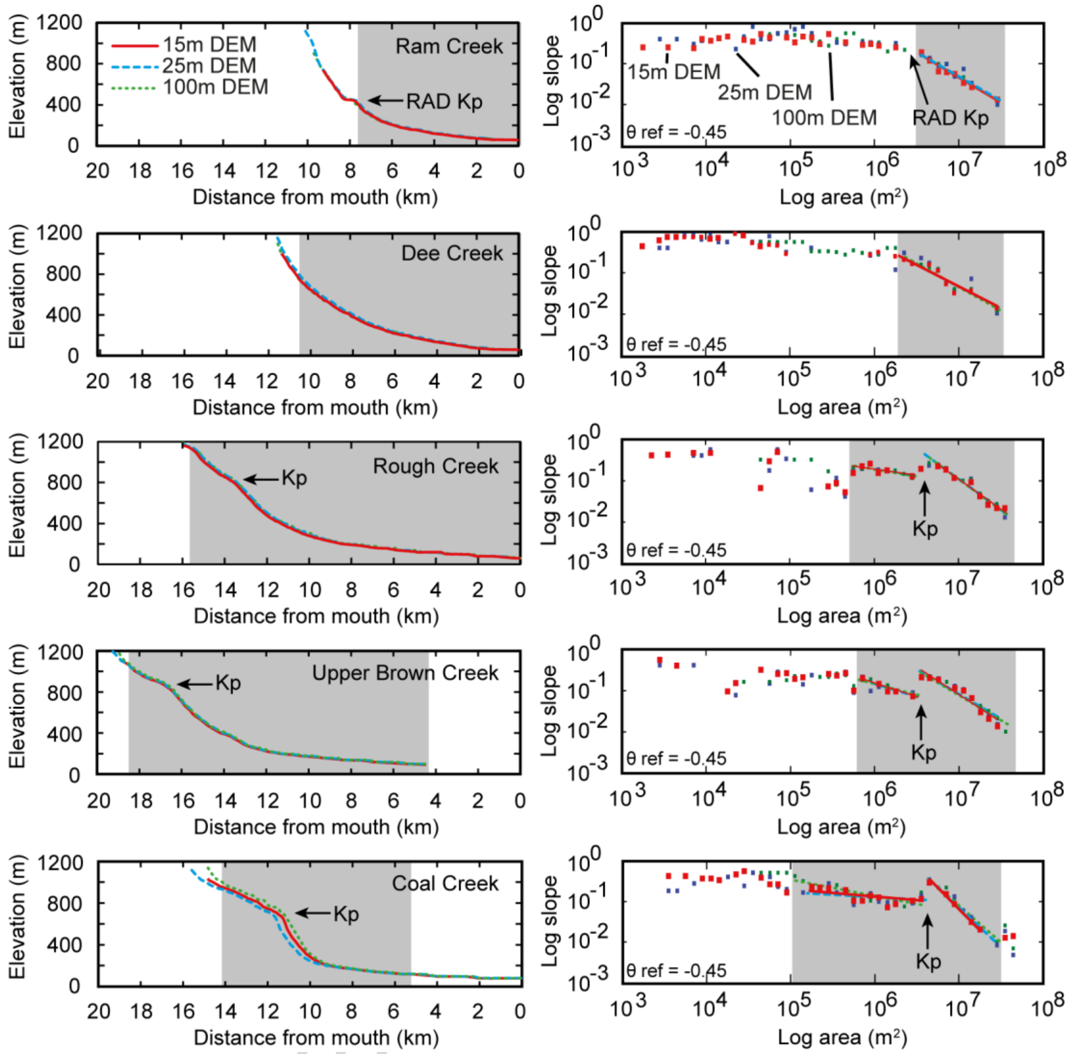

Elevation (m)
1200
800
400
0
20 18 16 14 12 10 8 6 4 2 0
Distance from mouth (km)
15m DEM
25m DEM
100m DEM
Ram Creek
RAD Kp
Dee Creek
Rough Creek
Kp
Upper Brown Creek
Coal Creek
Log slope
$10^0$
$10^{-1}$
$10^{-2}$
$10^{-3}$
$10^3$ $10^4$ $10^5$ $10^6$ $10^7$ $10^8$
Log area (m²)
θ ref = -0.45


Figure 7

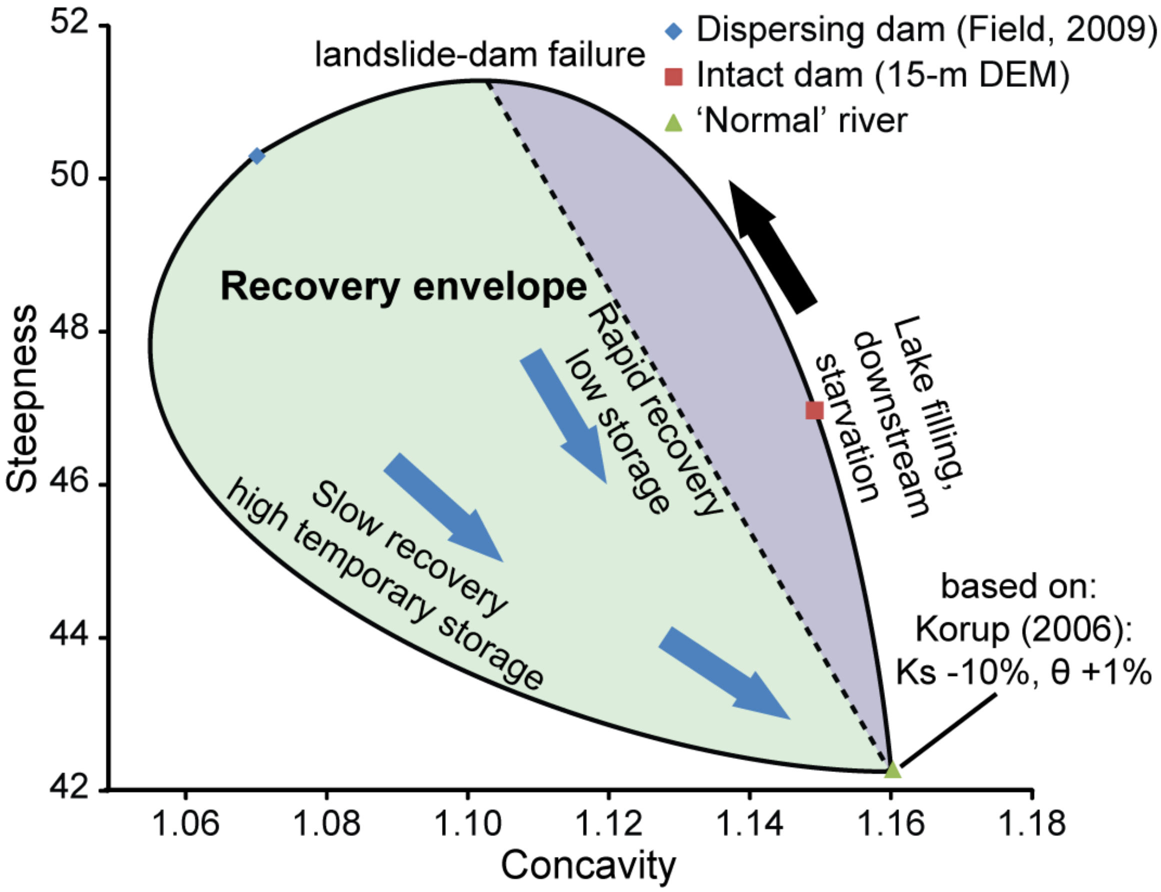

Dispersing dam (Field, 2009)
Intact dam (15-m DEM)
'Normal' river
landslide-dam failure
Recovery envelope
Rapid recovery
low storage
Slow recovery
high temporary storage
Lake filling,
downstream
starvation
based on:
Korup (2006):
Ks -10%, θ +1%
Steepness
Concavity
52
50
48
46
44
42
1.06
1.08
1.10
1.12
1.14
1.16
1.18


Figure 8

Table 1 $\Theta$ and $k_{sn}$ ($\Theta_{ref}$ = 0.45) indices for regressions over the whole river channel (including colluvial/fluvial/alluvial reaches), and fluvial only profile sections (excluding upstream colluvial and downstream alluvial sections) for five streams along the Brunner Range using profiles extracted from three differing resolution DEMs (15 m, 25 m, and 100 m).

| Creek name | DEM (m) | Whole profile | | Upstream fluvial | | Downstream fluvial | |
|---|---|---|---|---|---|---|---|
| | | $\theta$ | $k_{sn}$ | $\theta$ | $k_{sn}$ | $\theta$ | $k_{sn}$ |
| Ram | 15 | 0.29 ± 0.06 | 90.3 | | | 1.20 ± 0.26 | 78.9 |
| | 25 | 0.34 ± 0.06 | 97.4 | | | 1.10 ± 0.23 | 84.0 |
| | 100 | 0.5 ± 0.06 | 112.0 | | | 1.20 ± 0.21 | 79.1 |
| Dee | 15 | 0.32 ± 0.03 | 80.3 | | | 0.80 ± 0.13 | 96.9 |
| | 25 | 0.35 ± 0.04 | 88.3 | | | 1.00 ± 0.21 | 90.1 |
| | 100 | 0.51 ± 0.05 | 110.0 | | | 1.10 ± 0.15 | 89.3 |
| Rough | 15 | 0.27 ± 0.06 | 89.7 | 0.30 ± 0.23 | 96.4 | 1.40 ± 0.22 | 96.6 |
| | 25 | 0.26 ± 0.06 | 87.9 | 0.37 ± 0.22 | 96.0 | 1.50 ± 0.2 | 97.2 |
| | 100 | 0.36 ± 0.09 | 118.0 | 0.33 ± 0.19 | 96.6 | 1.50 ± 0.17 | 101.0 |
| Upper Brown | 15 | 0.28 ± 0.07 | 91.0 | 0.66 ± 0.23 | 65.9 | 1.30 ± 0.14 | 110.0 |
| | 25 | 0.29 ± 0.08 | 93.1 | 0.62 ± 0.32 | 63.9 | 1.20 ± 0.16 | 110.0 |
| | 100 | 0.33 ± 0.09 | 103.0 | 0.53 ± 0.15 | 68.3 | 1.20 ± 0.14 | 102.0 |
| Coal | 15 | 0.26 ± 0.08 | 86.1 | 0.19 ± 0.15 | 58.0 | 2.10 ± 0.22 | 156.0 |
| | 25 | 0.26 ± 0.08 | 82.0 | 0.12 ± 0.17 | 62.1 | 2.00 ± 0.23 | 147.0 |
| | 100 | 0.35 ± 0.10 | 103.0 | 0.40 ± 0.08 | 61.2 | 1.80 ± 0.19 | 143.0 |

Highlights

We examine nearly 30 years of post-landslide dam breach change
The system has not attained equilibrium and is transport limited
The river is eroding laterally instead of vertically keeping pace with uplift